Supporting Information for

Two Penta-Supertetrahedral Cluster-Based Chalcogenide Open Frameworks: Effect of Cluster Spatial Connectivity on Electron Transport Efficiency

Jing Lv,[†] Jiaxu Zhang,[†] Chaozhuang Xue,[†] Dandan Hu,[†] Xiang Wang,[†] Dong-Sheng Li,[‡] and Tao Wu*

[†] College of Chemistry, Chemical Engineering and Materials Science, Soochow University, Suzhou, Jiangsu 215123, China

[‡] College of Materials and Chemical Engineering, Hubei Provincial Collaborative Innovation Center for New Energy Microgrid, Key Laboratory of Inorganic Nonmetallic Crystalline and Energy Conversion Materials, China Three Gorges University, Yichang, Hubei 443002, China

E-mail: *wutao@suda.edu.cn*

Experimental Section

Materials. All analytical grade chemicals employed in this work were commercially available and used without further purification.

Synthesis of MCOF-1 and MCOF-2. A mixture of copper iodide (96 mg, 0.5 mmol), indium powder (114 mg, 1.0 mmol), sulfur powder (160 mg, 5.0 mmol), $SnCl_2$ (189 mg, 1.0 mmol), (*R*)(-)-2-amino-1-butanol (2-AB, 1.92 g, 21.6 mmol) and 1,8-diazabicyclo[5.4.0]-7-undecene (DBU, 1.96 g, 12.9 mmol) was stirred in a 23-mL Teflon-lined stainless steel autoclave for half an hour. The vessel was sealed and heated at 180 **°C** for 10 days, then the autoclave was cooled to room temperature. Red rod-like (**MCOF-1**) and red octahedron-like crystals (**MCOF-2**) were simultaneously obtained. Those raw products were washed three times by ethanol and filtered off, and 170 mg of purified crystals were obtained. Two phases were finally separated by hand. In addition, pure phase **MCOF-2** can also be prepared when 3 mL (2.94 g) of DBU was employed. Elemental analysis for **MCOF-1**, *calcd.* (*wt*%): C, 18.37; N, 4.79; H, 3.20; found: C, 18.18; N, 4.89; H, 3.01. Elemental analysis for **MCOF-2**, *calcd.* (*wt*%): C, 12.32; N, 3.50; H, 3.03; found: C, 12.22; N, 3.19; H, 2.14.

Single Crystal X-ray Diffraction (SCXRD). Single-crystal X-ray diffraction measurements were performed on Photon II CPAD diffractometer controlled using graphite-monochromated Mo-Kα (λ = 0.71073 Å) radiation at 120 K. The structure was solved by direct method using SHELXS-2014 and the refinements against all reflections of the compound were performed using SHELXS-2014.

Powder X-ray Diffraction (PXRD). PXRD data were collected on a desktop diffractometer (D2 PHASER, Bruker, Germany) using Cu-Kα (λ = 1.54184Å) radiation operated at 30 kV and 10 mA. The samples were ground into fine powders for several minutes before the test.

XPS and AES Measurements. X-ray photoelectron spectroscopy (XPS) and Auger electron spectroscopy (AES) were collected with a Leeman prodigy spectrometer

equipped with a monochromatic Al Kα X-ray source and a concentric hemispherical analyzer.

Alternating Current Impedance Spectroscopy (ACIS). ACIS characterization was measured by IM6 electrochemical workstation (Zahner Zennium, Germany) with a bias voltage near the open-circuit voltage (V_{oc}) of the sample in the 0.1M KOH electrolyte.

Elemental Analysis. Energy dispersive spectroscopy (EDS) analysis was performed on scanning electron microscope (SEM) equipped with energy dispersive spectroscopy detector. An accelerating voltage of 25 kV and 40 s accumulation time were applied. EDS results clearly confirmed the presence of Cu, In, Sn and S elements. Elemental analysis (EA) of C, H, and N was performed on VARIDEL III elemental analyzer.

Thermogravimetric Analysis (TGA). TGA measurement was performed with a Shimadzu TGA-50 system under nitrogen flow. The TG curve was performed by heating the sample from 20 to 800 °C with heating rate of 10 °C /min.

UV-Vis Absorption. Room-temperature solid-state UV-Vis diffusion reflectance spectra of crystal samples were measured on a SHIMADZU UV-3600 UV-Vis-NIR spectrophotometer coupled with an integrating sphere by using $BaSO_4$ powder as the reflectance. The absorption spectra were calculated from reflectance spectra by using the Kubelka-Munk function: $F(R)=\alpha/S=(1-R)^2/2R$, where R, α, and S are the reflection, the absorption and the scattering coefficient, respectively.

Fourier Transform Infrared Absorption. Fourier transform-Infrared spectral analysis was performed on a Thermo Nicolet Avatar 6700 FT-IR spectrometer with cesium iodide optics allowing the instrument to observe from 600-4000 cm^{-1}.

Ion Exchange. The samples of **MCOF-1** and **MCOF-2** (20 mg) were dipped in 20 mL aqueous solution of CsCl (1 M) in glass vial, which was slowly shaken by hand

for several seconds, then heated at 60 °C in oven. During treatment, the CsCl solution (1 M) was refreshed twice. After 12 hours, the crystals were taken out of solution and washed with water to remove residual Cs^+ ions adsorbed on the crystal surface.

Photoelectric Response. Typical preparation of film of **MCOF-1/ MCOF-2** on ITO electrode: 25.0 mg of ground **MCOF-1** or **MCOF-2** powder was dispersed in 50 mL isopropanol with the presence of 5.0 mg of $Mg(NO_3)_2 \cdot 6H_2O$. The sealed mixture suspension was continuously stirred for one day, and then was ultrasonically vibrated for half hour before electrophoretic deposition. The clean and sleek Pt plate electrode was used as anode, and the indium-tin-oxide (ITO) conductive glass as cathode. Constant working voltage was set up to 30 V. The whole electro-deposition process lasted for 30 minutes. The obtained ITO electrode decorated with **MCOF-1**/ **MCOF-2** film on its surface was finally washed with ethanol to remove residual isopropanol and $Mg(NO_3)_2$ salt left in suspension. The photocurrent experiments were performed on a CHI760E electrochemistry workstation in standard three-electrode configuration, with the sample coated ITO glass (the effective area is around 1 cm^2) as the working electrode, a Pt wire as the auxiliary electrode, and a saturated calomel electrode (SCE) as the reference electrode. The light source is a 150 W high pressure xenon lamp, located 20 cm away from the surface of the ITO electrode. Sodium sulfate aqueous solution (0.5 M, 100 mL) was used as the supporting electrolyte.

Resistivity Measurement. Samples (~120 mg) were first compressed into pellets with circular surface (s) of 1.327 cm^{-2} and thickness (L) of ~0.26−0.36 mm. The resistivity (ρ) of the sample was measured by ST2722-SZ semiconductor powder resistivity tester (Four-probe method).

Electrochemical Measurements. Electrochemical experiments were performed in a three-electrode electrochemical cell and conducted on a Rotating Disk Electrode (RDE) apparatus (RRDE-3A, BAS Inc.) equipped with computer-controlled CHI-760E. A rotating disk electrode (RDE) with a GC disk (4 mm in diameter) was used as working electrode. A KCl saturated no-leak Ag/AgCl electrode and a Pt plate

were used as the reference electrode and counter electrode, respectively. The procedure of pretreatment and modification of the working: electrode is as follows: it was firstly polished mechanically with 0.05 mm alumina slurry to obtain a mirror-like surface and then rinsed thoroughly with water, ethanol, and water and then allowed to dry. The homogeneous inks were prepared by dispersing 2 mg catalyst and 2 mg carbon black (CB) in mixture of 400 μL water, 100 μL ethanol and 20 μL 5% Nafion (5 *wt* % in propanol, Alfa Aesar) which were denoted as **MCOF-1**/**CB** and compound **2**/**CB**. The mixture was then sonicated strongly for 0.5 h to form a uniform ink 7 μL of as-prepared catalyst ink with catalyst loading of 0.437 mg·cm^{-2} was coated onto the pre-cleaned working electrode and dried at room temperature for the following electrochemical measurements. During the measurements, a gentle flow of O_2 or Ar_2 was maintained above the electrolyte. The background currents were collected in N_2-saturated electrolyte and corrected for the LSV under O_2. All the potentials used in this study were reported relative to the reversible hydrogen electrode (RHE).

Calculation Method.

The working electrode was scanned at a rate of 5 mV/s, while the ring electrode was set at 0.5 V (*vs*. Ag/AgCl) and rotated at 1600 rpm in 0.1MKOH. The H_2O_2 yield and electron transfer number (*n*) were calculated by following equations:

$$H_2O_2\% = \frac{200\frac{I_{ring}}{N}}{\frac{I_{ring}}{N} + I_{disk}}$$

$$n = \frac{4I_{disk}}{\frac{I_{ring}}{N} + I_{disk}}$$

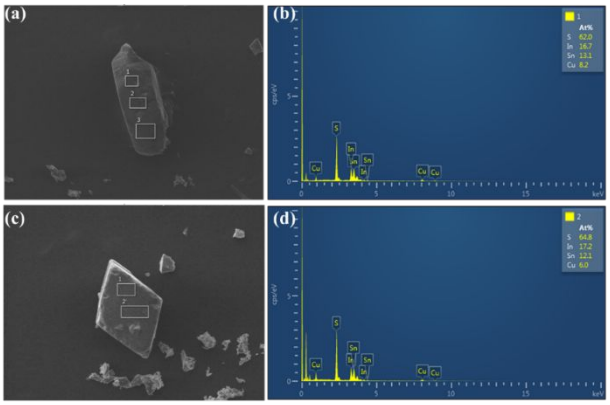

Figure S1. SEM images of as-synthesized **MCOF-1** (a) and **MCOF-2** (c), and energy dispersive spectroscopy (EDS) of **MCOF-1** (b) and **MCOF-2** (d).

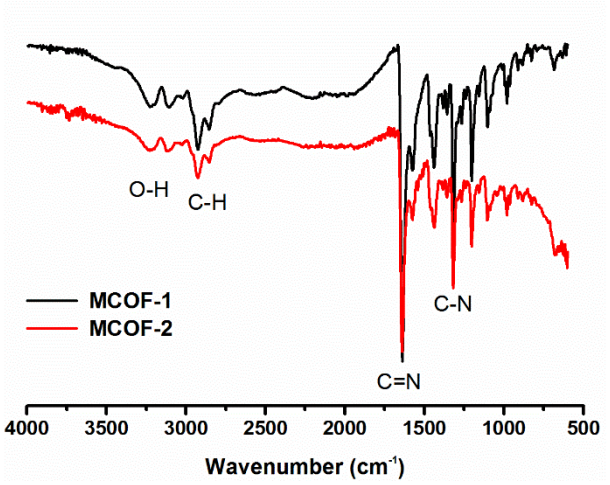

Figure S2. FT-IR spectra of **MCOF-1** and **MCOF-2.** The vibration bands of IR at about 1640 cm^{-1} indicate the presence of C=N of DBU. The IR bands at about 3230, 1320, 2930 cm^{-1} belong to the stretching vibrations of - OH, C - N, and C - H, respectively. The vibration at 1578 cm^{-1} was contributed by $-NH_2$ of 2-AB.

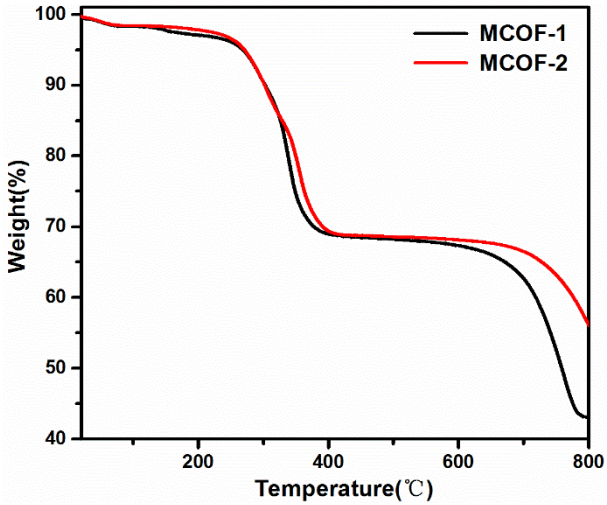

Figure S3. TGA curves of **MCOF-1** and **MCOF-2**.

Thermogravimetric (TG) analysis of **MCOF-1** shows two decomposition steps. The first weight loss of 1.95 % could be attributed to water molecules (*calcd*. 1.90 %). The second abrupt weight loss of around 29.05 % occurs between 140-400 **°C**, corresponding to removal of charge-balanced DBU and 2-AB molecules (*calcd.* 27.18 %). For **MCOF-2**, during the first step, about 1.8 % weight loss was observed from room temperature to 140 **°C**, which may be derived from loss of the co-crystallized water molecules (*calcd.* 2.0 %). During the second step, 29.0 % weight loss was detected from 140 **°C** to 410 **°C**, which is attributed to removal of DBU, 2-AB molecules and H_2S.

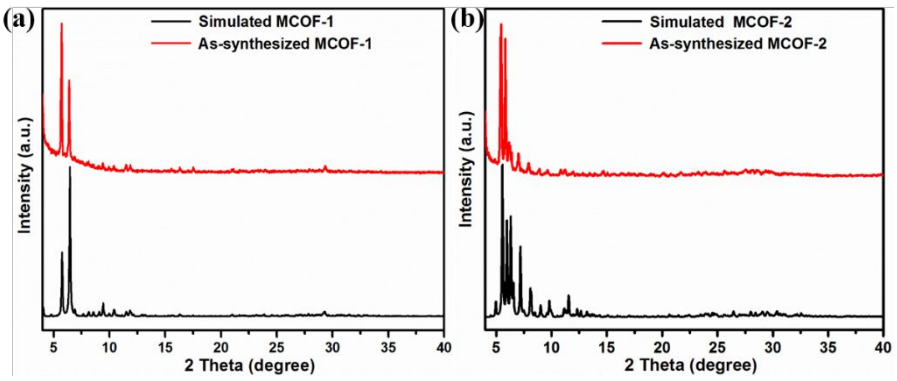

Figure S4. The simulated and experimental PXRD patterns of **MCOF-1** (a) and **MCOF-2** (b).

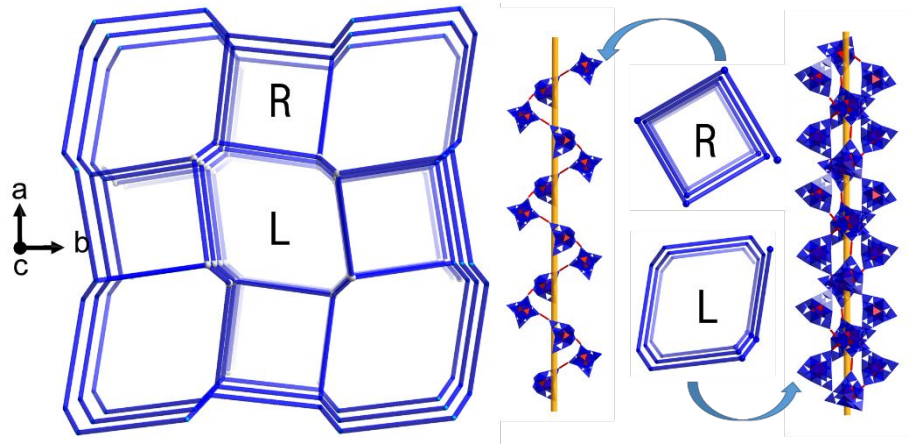

Figure S5. A *srs* topology in **MCOF-1** and the profile of helical chain.

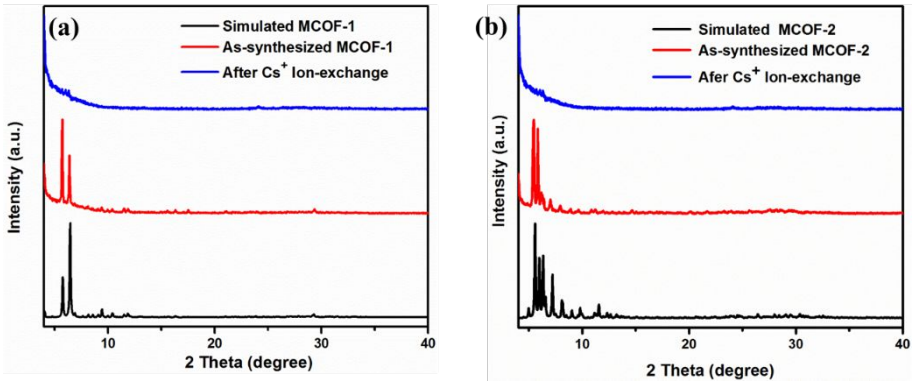

Figure S6. XRD patterns of MCOF-1 (a) and MCOF-2 (b) before and after ion-exchange.

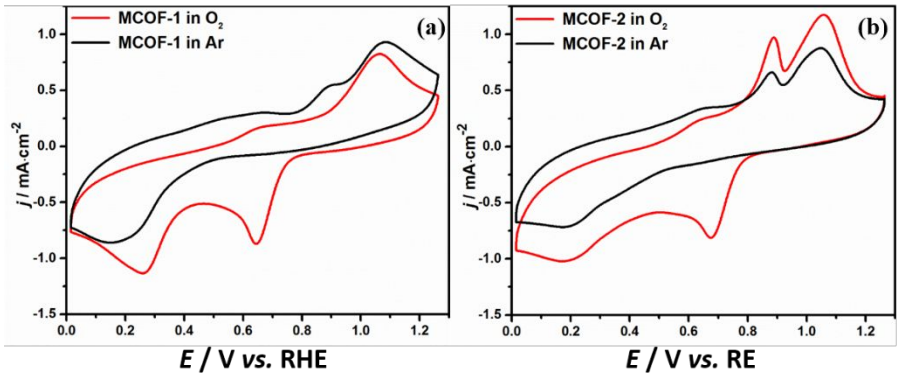

Figure S7. (a-b) Cyclic voltammograms (CVs) of **MCOF-1/CB** and **MCOF-2/CB** in Ar_2-(black) and O_2 (red) saturated 0.1 M KOH solution, scan rate: 50 mV/s.

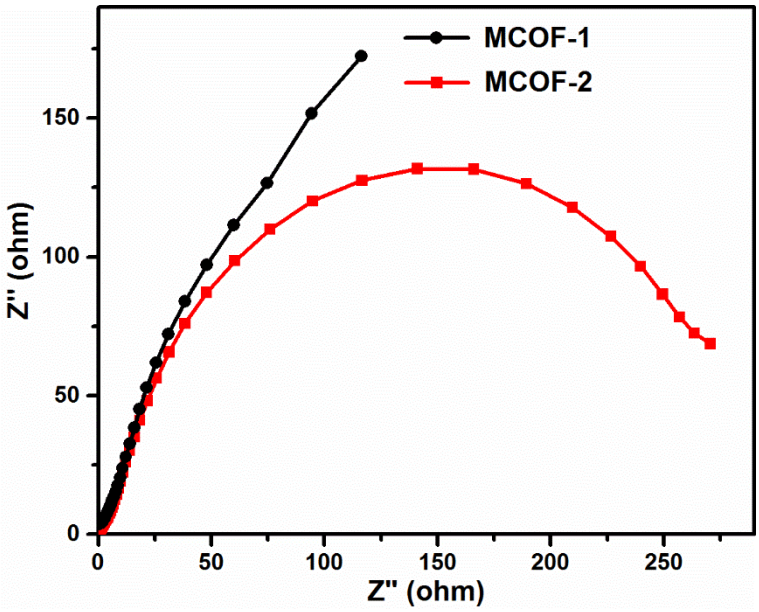

Figure S8. AC impedance plots of **MCOF-1** and **MCOF-2**.

Table S1. ICP-AES analysis of **MCOF-1** and **MCOF-2**.

Sample	Cu	In	Sn
MCOF-1	6.2	10.6	9.2
MCOF-2	6	12.5	7.5

Table S2. Crystallographic data and structure refinement parameters for **MCOF-1** and **MCOF-2**.

Compound	**MCOF-1**	**MCOF-2**
Formula	$[Cu_{24.8}In_{42.4}Sn_{36.8}S_{170}]$ $C_{347.2}H_{721.6}N_{77.6}O_{28}$	$[Cu_{12}In_{25}Sn_{15}S_{84}]$ $C_{103.6}H_{320.8}N_{26.6}O_{33}$
Crystal system	Tetragonal	Orthorhombic
Z	2	8
Space group	$P4_32_12$	*Pbca*
a /Å	30.298	27.4789
b /Å	30.298	29.7932
c /Å	34.98	39.8017
α /°	90	90
β /°	90	90
γ /°	90	90
V (Å^3)	32113	32585
D (g·cm^{-1})	2.347	2.169
μ (mm^{-1})	4.251	4.164
F (000)	14722	14668
R_{int}	0.1150	0.0839
GOF	1.146	1.014
R_1, wR_2 (I>2σ(I))	0.0659, 0.1648	0.0541, 0.1277
R_1, wR_2 (all data)	0.1060, 0.2059	0.0770, 0.1532